

Received April 23, 2019, accepted May 29, 2019, date of publication June 5, 2019, date of current version July 2, 2019.

Digital Object Identifier 10.1109/ACCESS.2019.2921003

Building Logistic Spiking Neuron Models Using Analytical Approach

LEI ZHANG¹, (Member, IEEE)

Faculty of Engineering and Applied Science, University of Regina, Regina, SK S4S 0A2, Canada

e-mail: lei.zhang@uregina.ca

ABSTRACT Spiking neuron models are inspired by biological neurons. They can simulate the neuronal activities of the mammalian brains, such as spiking (integrator) and periodic oscillation (resonator). A spiking neural network consisting of a cluster of spiking neurons can be used to simulate the collective dynamic behaviors of a brain neural network. This paper presents step-by-step analyses for the non-linear dynamics of mathematical spiking neuron models and sets forth a novel spiking model based on logistic function using an analytical approach. The logistic function is a well-known one-dimensional dynamical system and can generate spiking or periodic oscillation based on the system parameter. The novel spiking neural model is a combination of the integrate-and-fire and the quadratic integrate-and-fire neuron models with an added parameter to control the neural dynamics in order to generate stable, periodic, or chaotic neural behavior with flexibility. The analytical approach presented in this paper can be applied extensively to the design and analyses of multi-dimensional neuron models. The goal of this research project is to understand the dynamical behaviors of biological neurons in order to design biologically inspired spiking neuron model for building artificial intelligence, treating cognitive disorders, and advancing the scientific frontiers of brain research.

INDEX TERMS Analytical models, bifurcation, chaos, nonlinear dynamical systems, logistic map, logistic function, spiking neural model, integrate-and-fire, quadratic integrate-and-fire, differential equations.

I. INTRODUCTION

Spiking is a discrete event that assimilates a neuronal firing in the brain. Spiking neural network (SNN) has ultra-low power implementation in hardware due to sparsity, and time-based encoding. A spiking neuron model uses differential equations to represent various neuronal activities. Some of these activities can lead to the generation of action potential, which is the charge in electrical potential (voltage) associated with a neuron. When a neuron reaches a certain threshold, it spikes, and the potential of the neuron resets. A popular simple neuron model is proposed by [1]; a hybrid spiking neuron model is introduced in [2]; and a number of spiking neuron models are discussed in [3]. Although these models are all plausible and have been used either to simulate major neuronal dynamical behaviors or to build large scale spiking neural networks, none of them has been used to analytically model the chaotic behaviors of a dynamical system with controllable system parameters. This has led to the endeavor taken in this research

to build generalized spiking neuron models based on logistic function using analytical approach. Logistic map is a one dimensional dynamical system which demonstrates chaotic features [4]. It can be used as a discrete-time demographic model to predict the population of a species. The logistic function, the continuous counterpart of the discrete logistic map, can be represented by differential equations.

A neuron has three major components: a cell body, an axon, and dendrites, as illustrated in Fig. 1. A neuron receives electrical currents from other neurons through its many dendrites; accumulates electrical potential within its cell body; and generates an action potential passing down its axon; at the end of the axon, synapses form between the axon and dendrites of the same neuron and other neurons. Computational intelligence models have been developed to form a better understanding of the details of neuronal and neural functions [5]. The main goal of this research is to design generalized spiking neuron models based on logistic function, that is, to resemble the dynamical properties of logistic map.

The rest of the paper is structured as follows: section II compares the dynamical properties of two common spiking

The associate editor coordinating the review of this manuscript and approving it for publication was Ho Ching Iu.

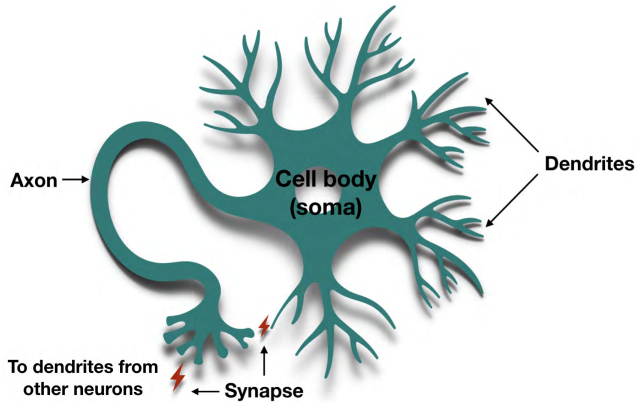


FIGURE 1. Biological neuron components.

neuron models: the integrate-and-fire model and the quadratic integrate-and-fire model; section III demonstrates the dynamical behaviors of the discrete logistic map and the continuous logistic function; section IV presents a generalized spiking neuron model based on the logistic function, by combining the integrate-and-fire model and the quadratic integrate-and-fire model; and Section V discusses the conclusion and future work.

II. SPIKING NEURON MODELS

Spiking neuron models are more biologically plausible than classical neuron models, which involve weight multiplication and sigmoidal activation function [3]. Artificial neural networks (ANN) built with classical neuron models inevitably incur high computational cost and long training time, despite that much research effort has been put into improving the training performance by optimizing either the ANN architectures [6], [7] or the quality of the training data [8]–[10]. In comparison, spiking neuron models are binary models and can be more computational efficient, potentially more suitable for simulating large scale neural networks. Although the summation and thresholding prior to spiking is, in both nature and modeling, an analog function. The output of a spike can, however, be represented digitally. A bioinspired binary oscillator is presented in the US patent [11] and related publication [12]. Two common spiking neuron models: the integrate-and-fire model and the quadratic integrate-and-fire model are discussed and compared using analytical approach. They are represented mathematically by one dimensional differential equations and their dynamical properties, such as stability and oscillation, can be controlled by a single system parameter.

A. LEAKY INTEGRATE-AND-FIRE (LIF) NEURON MODEL

A widely used spiking neuron model is the Leaky integrate-and-fire (LIF) model. The dynamics of the membrane potential in the LIF neuron are described by a single first-order linear differential equation (1).

$$C \frac{dV(t)}{dt} + \frac{V(t)}{R} = I(t) \quad (1)$$

where C is the membrane capacitance, R is the resistance, V is the voltage and I is the current. In the LIF model, the neuronal membrane voltage potential is modeled as an exponentially attenuating RC oscillatory system with a time constant τ . The attenuation of the neuronal membrane voltage potential can be mathematically represented in (2), where Δt is the time step.

$$V_{mem}(n+1) = V_{mem}(n) \cdot e^{-\Delta t/\tau}, \quad \tau = RC \quad (2)$$

The LIF model can be used to represent a neuron with leakage current and gated current in (3). The voltage sensitive current is activated instantaneously when the membrane potential V reaches a certain threshold, and the neuron fires an action potential, while V is reset to the resting potential.

$$C \dot{V} = I - g_L(V - V_L) \quad (3)$$

A simplified equation can be derived from the LIF model by rescaling as listed in (4), where $v_{peak} = 1$ is the threshold; $v_{reset} = 0$ is the reset value; v is between zero and one ($v \in [0, 1]$). Let $\dot{v} = f(v)$, the fixed points are the solutions of $f(v) = b - v = 0$, hence $v^* = b$ is the equilibrium, i.e., the rest state, which corresponds to the state where the membrane voltage v does not change. The eigenvalue (λ) is defined as $\lambda = f'(v)$. The equilibrium is stable if the eigenvalue is negative $f'(v) < 0$, i.e., $f(v)$ changes from positive to negative as v increases around v^* . Since the $f(v)$ is a monotonically decreasing line, with a negative slope $f'(v) = -1$, the equilibrium is stable.

$$f(v) = \dot{v} = b - v, \quad \text{if } v = 1, \text{ then } v \leftarrow 0 \quad (4)$$

The solution to $\dot{v} = b - v$ with $v(0) = 0$ is $v(t) = b(1 - e^{-t})$. When $b < 1$, the neuron is excitable and can generate a single spike; When $b > 1$, the neuron resonates and fire periodic spike trains at period $T = -\ln(1 - 1/b)$, determined from the threshold crossing $v(T) = 1$, as derived in (5). And the general solution with $v(0) = v_0$ is derived in (6).

$$\begin{aligned} \frac{dv}{dt} = b - v &\Rightarrow \frac{dv}{b - v} = dt \Rightarrow \int \frac{dv}{b - v} = \int dt \\ \text{Let } u = b - v, \text{ then } du = -dv & \\ \Rightarrow \int -\frac{1}{u} du = \int dt &\Rightarrow -\ln|u| = t + c \\ \Rightarrow -\ln|b - v| = t + c & \\ \Rightarrow v(t) = b - e^{-(t+c)} = b - e^{-c}e^{-t} & \end{aligned} \quad (5)$$

Special solution:

Let $v(0) = 0$, then $e^{-c} = b$, $v(t) = b - b \cdot e^{-t}$

Let $v(T) = 1$, then $1 = b(1 - e^{-T})$

$$\Rightarrow T = -\ln|1 - \frac{1}{b}|$$

General solution:

Let $v(0) = v_0$, Then $e^{-c} = b - v_0$,

$$v(t) = b - (b - v_0) \cdot e^{-t}$$

Let $v(T) = v_{peak}$,

$$\text{Then } \Delta v = v_{peak} - v_{reset} = b - (b - v_0)e^{-T}$$

$$\Rightarrow T = -\ln \left| \frac{b - \Delta v}{b - v_0} \right| \quad (6)$$

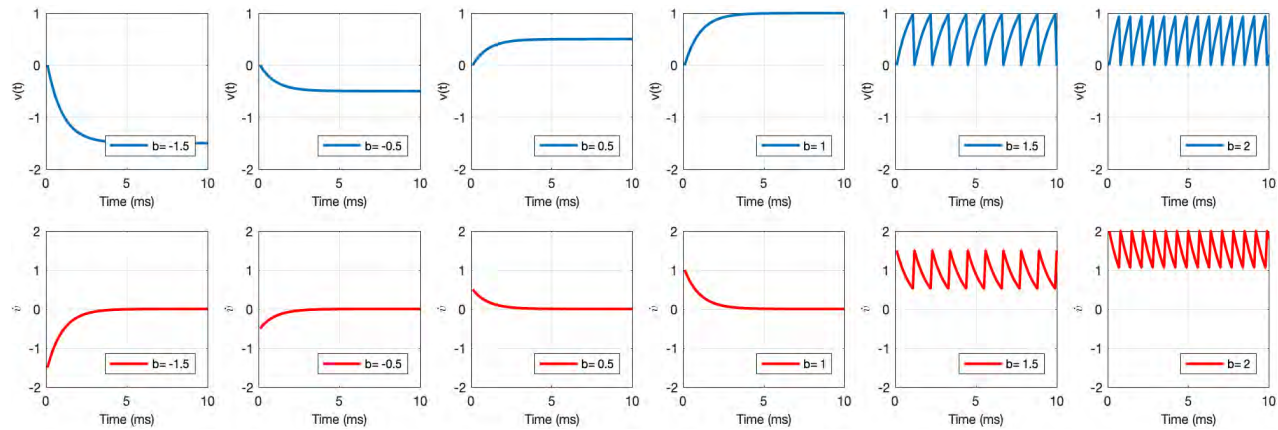


FIGURE 2. Excitation of the integrate-and-fire model.

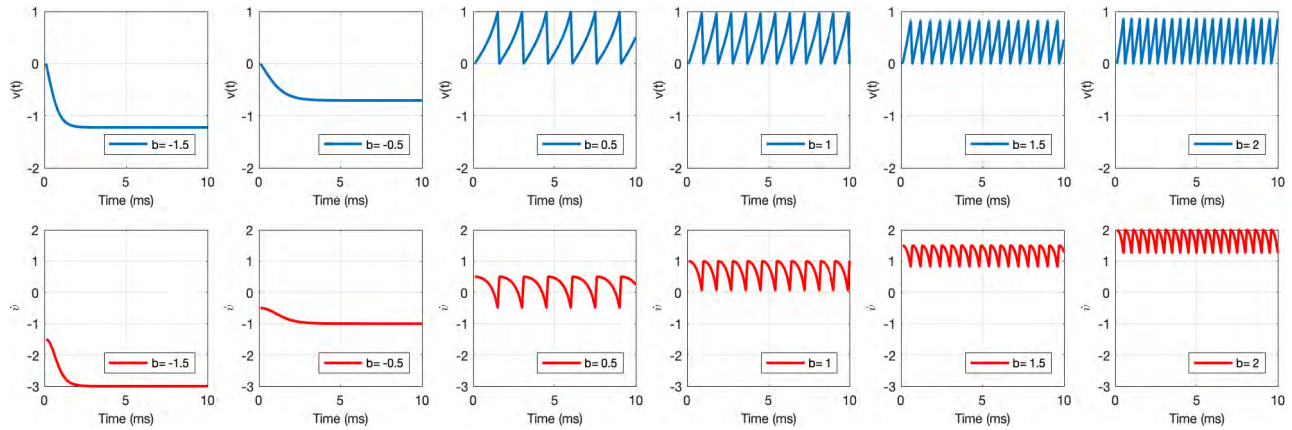


FIGURE 3. Excitation of the quadratic-integrate-and-fire model.

The integrate-and-fire model has a number of computational properties. The $v(t)$ and $v'(t)$ at a number of different b values are shown in Fig. 2. The different values of b are selected in order to demonstrate different excitatory behaviors of the neuron. When $b < v_{peak}$, $v(\infty)$ converges to b , i.e., $v(\infty) = b$. When $b < v_{peak}$, v resonates periodically between v_{reset} and v_{peak} , in which case the frequency of the spiking is proportional to b , and the amplitude of the spiking is inversely proportional to b . The size and period of all spikes for a given value of b are assumed to be the same. Positive input current $b > 0$ can increase membrane potential and cause the neuron to fire a spike; while negative input current $b < 0$ inhibits spike generation. The model demonstrates Class 1 excitability, i.e., the frequency of the spiking can be modulated by the input current. Strictly speaking, the leaky integrate-and-fire model should not be considered as a spiking neuron model since it does not have an intrinsic spike generating mechanism. The spike is manually coded into the model instead of generated by the model. Nevertheless, the model is regarded as a mathematical model with good computational efficiency but unsuitable for simulating large-scale network for computational neuroscience due to its insufficiency in modeling various neuronal behaviors [13].

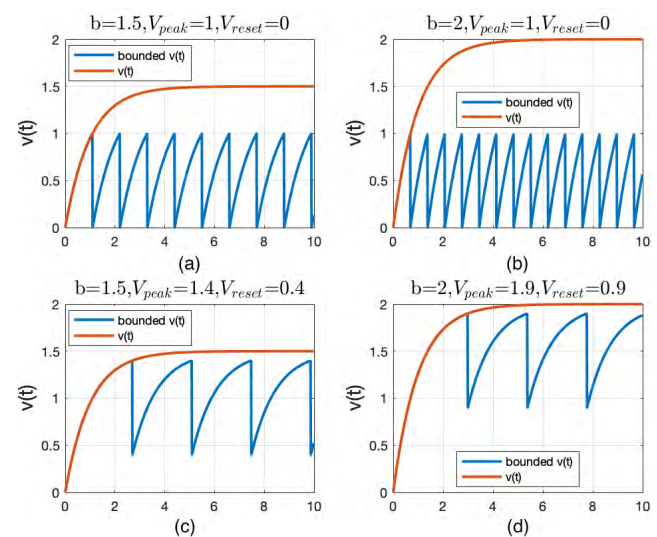


FIGURE 4. Parameters of integrate-and-fire model. (a) $b = 1.5$, $V_{peak} = 1$, $V_{reset} = 0$. (b) $b = 2$, $V_{peak} = 1$, $V_{reset} = 0$. (c) $b = 1.5$, $V_{peak} = 1.4$, $V_{reset} = 0.4$. (d) $b = 2$, $V_{peak} = 1.9$, $V_{reset} = 0.9$.

Analytically, the parameter b of the integrate-and-fire model defines the rising speed of the spike, as shown in Fig. 4(a) and (b), where $v_{reset} = 0$, $v_{peak} = 1$. The red plot

indicates the solution of the differential equation $v(t)$. The blue plot indicates the periodic spiking generated with the boundary conditions, i.e., when $v(t) > v_{peak}$, $v(t) \leftarrow v_{reset}$. The bigger the value of b , the faster the spike reaches v_{peak} , corresponding to shorter period (T) and faster spiking frequency. The spiking frequency also depends on the difference between v_{peak} and v_{reset} , denoted as Δv . Given the same initial state (v_0), the bigger the value of Δv , the longer the period, and the lower the spiking frequency. On the other hand, when the initial value changes, the frequency changes accordingly based on the rising time of the segment between v_{peak} and v_{reset} on the $v(t)$ curve. For instance, Fig. 4(c) shows the periodic spiking generated with $v_{reset} = 0.4$, $v_{peak} = 1.4$, $b = 1.5$. The Δv equals 1, which is the same as Fig. 4(a), but the spiking frequency is much slower. Similarly, in Fig. 4(d), with $v_{reset} = 0.9$, $v_{peak} = 1.9$, $b = 2$, Δv also equals 1, but the spiking frequency is much slower than Fig. 4(b).

B. QUADRATIC INTEGRATED-AND-FIRE MODEL

The quadratic integrate-and-fire model represented by the differential equation (7) can be used to describe the saddle-node bifurcation of the more comprehensive four dimensional Hodgkin-Huxley neuron model [14]. The solution to the equation is derived as listed in (8). At the given initial condition $v(0) = 0$, the constant $C = 0$. The period of the spiking is listed in (9). The frequency is proportional to \sqrt{b} . The $v(t)$ and $\dot{v}(t)$ at a number of different b values are shown in Fig. 3, with $v_{reset} = 0$, and the initial voltage $v_0 = 0$. If $b > 0$, then $\dot{v} > 0$, v increases till it reaches v_{peak} and reset to v_{reset} . If $b < 0$, $\dot{v} = b + v^2 = 0$ has two real solutions, therefore the model has two equilibria at $\pm\sqrt{|b|}$, corresponding to the stable (rest) and unstable (firing threshold) states respectively. The $\dot{v} - v$ plot of the quadratic model is show in Fig. 6.

$$\dot{v} = b + v^2, \quad \text{if } v = v_{peak}, \text{ then } v \leftarrow v_{reset} \quad (7)$$

Given the derivative of trigonometric function:

$$\tan'(x) = 1 + \tan^2(x)$$

$$\text{Let } \frac{v}{\sqrt{b}} = \tan(u), \rightarrow u = \tan^{-1}\left(\frac{v}{\sqrt{b}}\right) = \text{atan}\left(\frac{v}{\sqrt{b}}\right)$$

$$\text{Then } dv = \sqrt{b} * \tan'(u) = \sqrt{b} * \left(1 + \tan^2(u)\right)$$

$$\frac{dv}{dt} = v^2 + b = b * \left(1 + \left(\frac{v}{\sqrt{b}}\right)^2\right) = b * \left(1 + \tan(u)^2\right)$$

$$\Rightarrow du = \sqrt{b} dt, \rightarrow \int du = \int \sqrt{b} dt$$

$$\Rightarrow v(t) = \sqrt{b} * \tan\left(\sqrt{b} * (t + C)\right), \quad C \text{ is a constant}$$

$$\text{Let } v(0) = v_0, \quad \text{then } C = \frac{1}{\sqrt{b}} \text{atan} \frac{v_0}{\sqrt{b}} \quad (8)$$

$$T = \frac{1}{\sqrt{b}} \left(\text{atan} \frac{v_{peak}}{\sqrt{b}} - \text{atan} \frac{v_{reset}}{\sqrt{b}} \right) < \frac{\pi}{\sqrt{b}} \quad (9)$$

In Fig. 5, the solution of the differential equation $v(t)$ is plotted in red, and the bounded $v(t)$ generated with boundary conditions v_{peak} and v_{reset} using Euler method is plotted

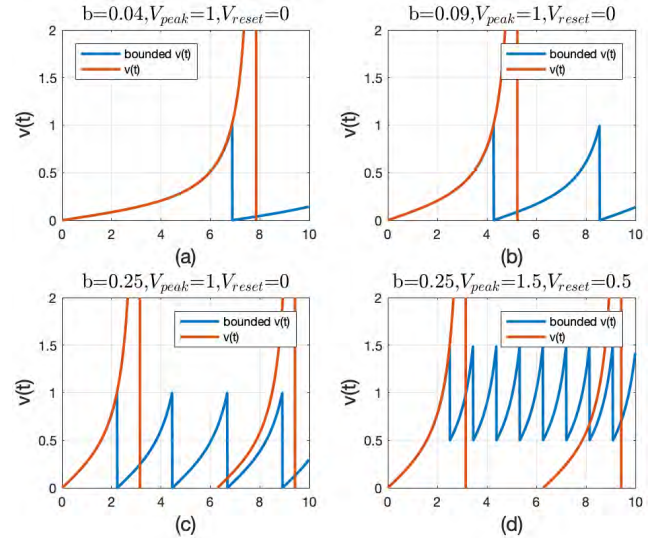


FIGURE 5. Parameters of quadratic integrate & fire model. (a) $b = 0.04$, $V_{peak} = 1$, $V_{reset} = 0$. (b) $b = 0.09$, $V_{peak} = 1$, $V_{reset} = 0$. (c) $b = 0.25$, $V_{peak} = 1$, $V_{reset} = 0$. (d) $b = 0.25$, $V_{peak} = 1.5$, $V_{reset} = 0.5$.

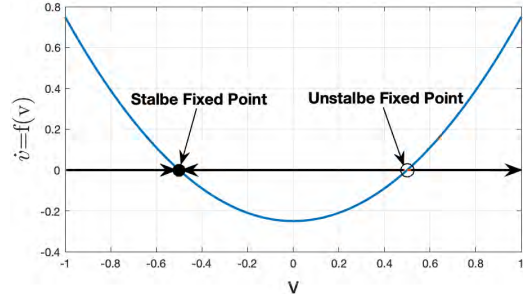


FIGURE 6. Stability of the quadratic integrate and fire model.

in blue. The rising speed of the spike depends on the parameters b , v_{peak} , and v_{reset} . With the same v_{peak} , and v_{reset} , the bigger b is, the shorter time for the spike to ramp from v_{reset} to v_{peak} , and hence the higher spiking frequency, as being observed by comparing Fig. 5(a) and (b). With the same b , the spiking frequency depends on the reset state v_{reset} and Δv , i.e., the difference between v_{reset} and v_{peak} . Additionally, with the same v_{reset} , the bigger the v_{peak} , the longer the rising time, and hence the slower the frequency. With the same b and Δv , the frequency solely depends on v_{reset} , as depicted by Fig. 5(c) and (d).

Subthreshold perturbation occurs when v is smaller than the unstable equilibrium; while superthreshold perturbation occurs when v is pushed bigger than the unstable equilibrium resulting in the generation of a spike. The subthreshold and superthreshold perturbations are illustrated in Fig. 7, where $b = 0.25$. The stable equilibrium is at $v = -\sqrt{|b|} = -0.5$, and the unstable equilibrium is at $v = \sqrt{|b|} = 0.5$. When $v_0 = 0.4$, subthreshold perturbation occurs; when $v_0 = 0.6$, superthreshold perturbation occurs. Since $v_{reset} = 0$ is smaller than the unstable equilibrium $\sqrt{|b|}$, i.e., $v_{reset} < \sqrt{|b|}$, in both cases, the $v(\infty)$ converges to the stable equilibrium(-0.5). When $v_{reset} < 0$, the model is monostable. When $v_{reset} > 0$, it could be bistable; and typically

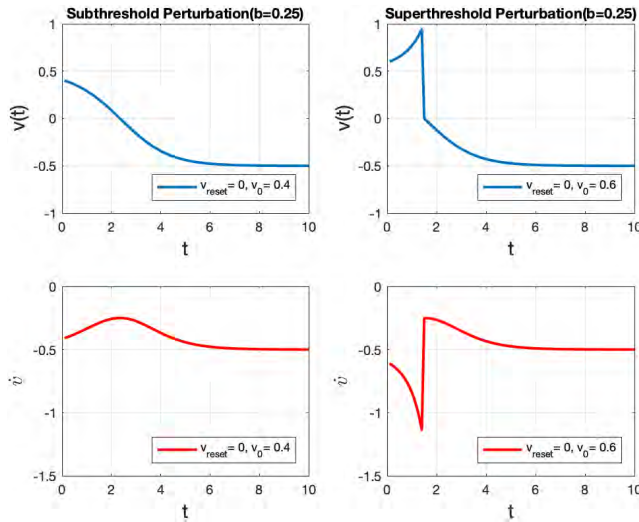


FIGURE 7. Subthreshold and superthreshold perturbations of the quadratic integrate and fire model.

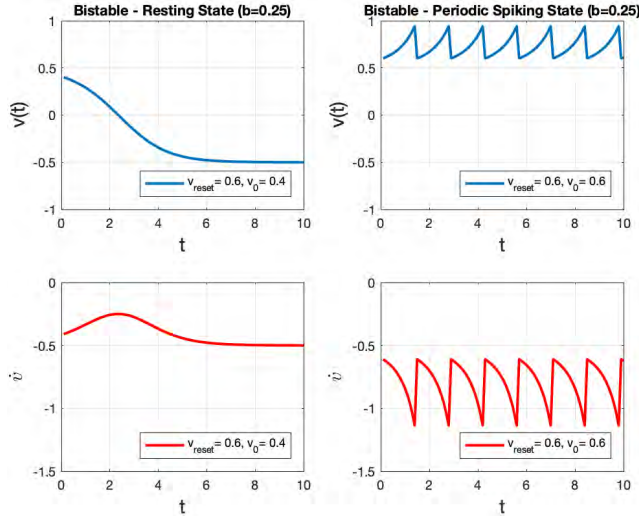


FIGURE 8. Bistable states of the quadratic integrate and fire model.

when v_{reset} is bigger than the unstable equilibrium(+0.5), i.e., $v_{reset} > \sqrt{|b|}$, the model is bistable between the resting state and the periodic spiking state. The bistable states are illustrated in Fig. 8, where $b = 0.25$, $v_{reset} = 0.6$. When the initial state $v_0 = 0.4$, which is smaller than the unstable equilibrium $\sqrt{|b|} = 0.5$, $v(\infty)$ converges to the resting state at the stable equilibrium (-0.5); When $v_0 = 0.6$, which is greater than the unstable equilibrium (+0.5), the model generates periodic spiking.

III. DYNAMICAL BEHAVIORS OF DISCRETE LOGISTIC MAP AND CONTINUOUS LOGISTIC FUNCTION

A. DISCRETE LOGISTIC MAP

The discrete logistic map equation is listed in (10). It has two fixed points (equilibria), which are listed in (11) together with the stability of the fixed points based on system parameter [15]. x_n is the variable whose value is between zero and

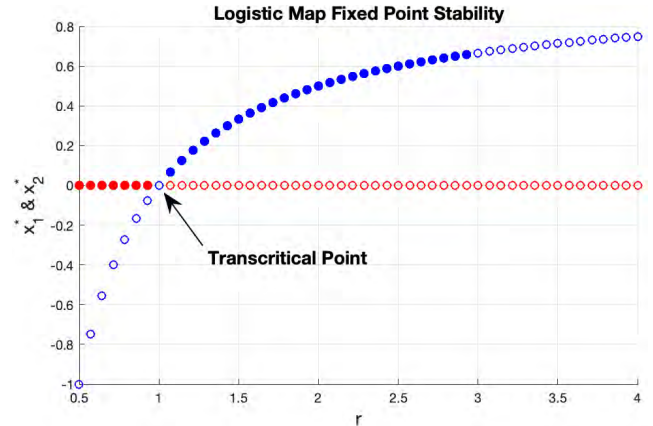


FIGURE 9. Logistic map stability based on parameter r .

one ($x_n \in [0, 1]$). r is the system parameter r with a range of interest between 0 and 4 for dynamical analysis. The fixed points are the solutions of $x_{n+1} = x_n$. The derivative of x is $x' = f(x)$, if $|f(x^*)| < 1$, the fixed point is stable; if $|f(x^*)| > 1$, the fixed point is unstable. It can be derived that the fixed point x_1^* is stable when $r < 1$, and the fixed point x_2^* is stable when $1 < r < 3$. When $r = 1$, $x_1^* = x_2^* = 0$, the two fixed points exchange stability. This phenomenon is called transcritical bifurcation, which is a common type of bifurcations in dynamical system. Fig. 9 shows the stability of two fixed points at different r value. x_1^* is plotted in red, and x_2^* is plotted in blue. Solid circle indicates stable fixed point, while hollow circle indicates unstable fixed point.

$$x_{n+1} = rx_n(1 - x_n) = -rx_n^2 + rx_n \quad (10)$$

Fixed points:

$$x_{n+1} = rx_n(1 - x_n) = x_n$$

$$x_{n+1} - x_n = rx_n(1 - x_n) - x_n = 0$$

$$\Rightarrow \begin{cases} x_1^* = 0 \\ x_2^* = 1 - \frac{1}{r} \end{cases}$$

Fixed points stability:

$$\begin{cases} |f(x_1^*)| = |r(1 - 2x_1^*)| = r < 1 \\ |f(x_2^*)| = |r(1 - 2x_1^*)| = |2 - r| = < 1 \end{cases} \quad (11)$$

The bifurcation of the logistic map with the initial value $x_0 = 0.2$ and the parameter r ranging from -2 to 4 is plotted in Fig. 10. In addition to the two fixed point values, if the initial value $x_0 = 1$, then the next value $x_{n+1} = 0$, which is a fixed point. There are two bifurcation points at $r = -1$ and $r = 1$, where $x(n)$ changes from stable state (single value) to periodic state (oscillating between two values). Fig. 11 further demonstrates the dynamical characteristics of the discrete logistic map with different r values. As r increases from -2 to 4, the stability of the logistic map outputs $x(n)$ varies accordingly, as explained in details below.

- $r = -2$: $x(n)$ is in a chaotic unstable state, its values are random between -0.5 and 1.5. As r decreases from

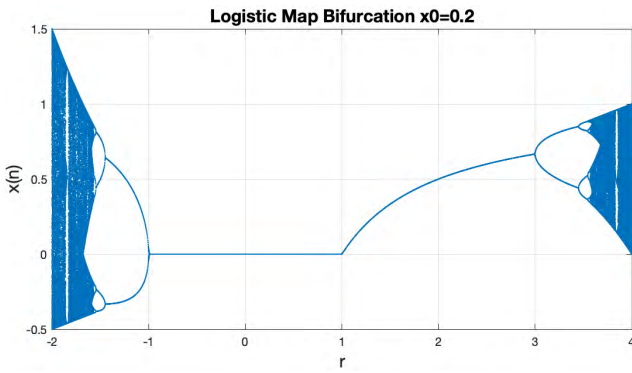


FIGURE 10. Logistic map bifurcation.

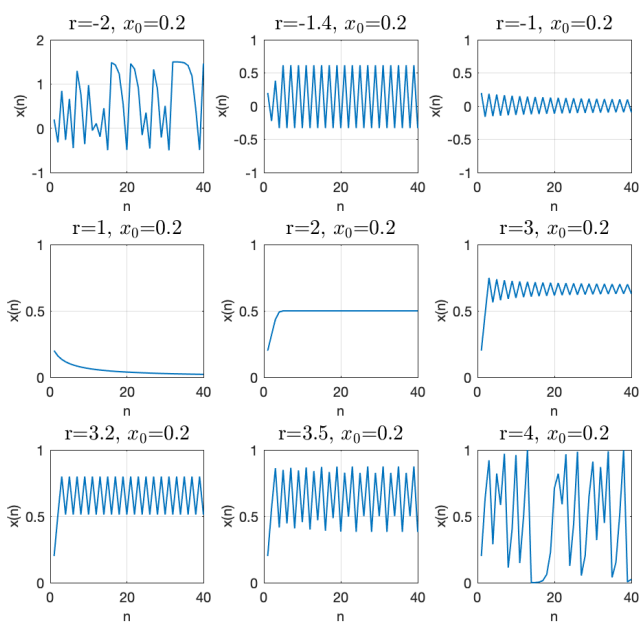


FIGURE 11. Parameter r of the discrete logistic map.

-1 to -2 , $x(n)$ goes through period doubling sequentially with periods of $2, 4, 8$, etc., and quickly becomes chaotic.

- $r = -1.4$: $x(n)$ is periodic with a period of two, it oscillates between two stable values.
- $r = -1$: This is a bifurcation point separating two states: a stable state with a single value and a periodic state with oscillation between two values. As the initial value $x_0 = 0.2$, $x(n)$ oscillates with attenuation towards equilibrium at $x(n) = 0$. As r increases from -1 to 1 , $x(n)$ converges to the stable fixed point at $x(n) = 0$.
- $r = 1$: This is a transcritical point, as r increases from 1 to 3 , $x(n)$ converges to the stable fixed point at $x(n) = 1-1/r$.
- $r = 2$: $x(n)$ converges to the fixed point at $x(n) = 0.5$.
- $r = 3$: This is another bifurcation point. As the initial value $x_0 = 0.2$, $x(n)$ oscillates with attenuation towards equilibrium at $x(n) = 1-1/r = 2/3$. As r increases from 3 to 4 , $x(n)$ goes through period doubling

sequentially with periods of $2, 4, 8$, etc., and quickly becomes chaotic.

- $r = 3.2$: $x(n)$ is periodic with a period of two, it oscillates between two values.
- $r = 3.5$: $x(n)$ is periodic with a period of four, it oscillates sequentially among four values.
- $r = 4$: $x(n)$ is in a chaotic unstable state, its values are random between -1 and 1 .

B. CONTINUOUS LOGISTIC DIFFERENTIAL EQUATION

The continuous logistic differential equation and the steps for deriving its solution are listed in (12).

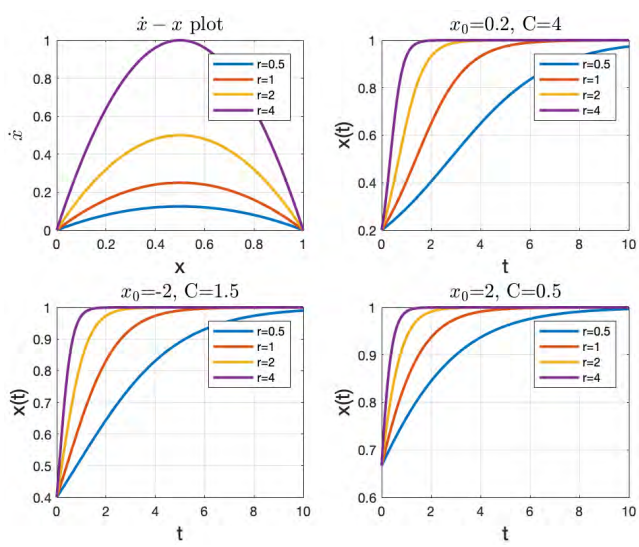


FIGURE 12. Logistic function parameters and initial values.

Fig. 12 (top left) shows the $\dot{x} - x$ curves for four selected values of parameter r ($0.5, 1, 2, 4$). There are two fixed points where $\dot{x} = 0$. $x = 0$ is an unstable fixed point as $\dot{x} > 0$ at the fixed point; while $x = 1$ is a stable fixed point as $\dot{x} < 0$ at the fixed point. As $x(t) = \frac{1}{Ce^{-rt}+1}$ and $C = |\frac{1}{x_0} - 1|$, the solutions to the logistic differential equation can be different depending on the initial value x_0 , as explained in details below.

- When $x_0 = 0$ (unstable fixed point) $\Rightarrow \frac{1}{x_0} \rightarrow \infty \Rightarrow C = \frac{1}{x_0} - 1 \rightarrow \infty \Rightarrow x(t) \rightarrow 0$.
- When $x_0 = 1$ (stable fixed point) $\Rightarrow C = \frac{1}{x_0} - 1 = 0 \Rightarrow x(t) = 1$.
- When $0 < x_0 < 1 \Rightarrow \frac{1}{x_0} > 1 \Rightarrow C = \frac{1}{x_0} - 1 > 0$, $x(t)$ converges to the stable fixed point ($x^* = 1$) as t increases. An example with $x_0 = 0.2, C = 4$ is shown in Fig. 12 (top right).
- When $x_0 < 0 \Rightarrow \frac{1}{x_0} < 0 \Rightarrow C = \frac{1}{x_0} - 1 < -1$, $x(t)$ also converges to the stable fixed point ($x^* = 1$) as t increases. An example with $x_0 = -2, C = 1.5$ is shown in Fig. 12 (bottom left).
- When $x_0 > 1 \Rightarrow 0 < \frac{1}{x_0} < 1 \Rightarrow C = \frac{1}{x_0} - 1 \in (-1, 0)$, $x(t)$ converges to the stable fixed point ($x^* = 1$)

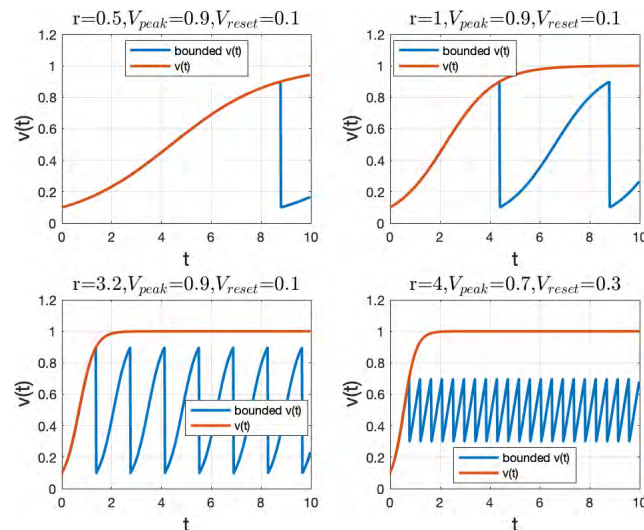


FIGURE 13. Parameters of logistic integrate-and-fire model.

as t increases. An example with $x_0 = 2$, $C = 0.5$ is shown in Fig. 12 (bottom right).

$$\begin{aligned} \dot{x} &= \frac{dx}{dt} = rx - rx^2 = rx(1-x) \\ \Rightarrow \frac{1}{x(1-x)} \frac{dx}{dt} &= r \Rightarrow \left(\frac{1}{x} + \frac{1}{1-x}\right) \frac{dx}{dt} = r \\ \Rightarrow \int_x^1 \left(\frac{1}{x} - \frac{1}{1-x}\right) dx &= \int_t^r dt \\ \Rightarrow \ln|x| - \ln|1-x| &= r \cdot t + C_1 \\ \Rightarrow \ln \left| \frac{x}{1-x} \right| &= r \cdot t + C_1 \\ \text{If } \frac{x}{1-x} > 0 \rightarrow 0 < x < 1 \\ \Rightarrow \frac{x}{1-x} &= e^{r*t+C_1} = e^{C_1} \cdot e^{rt} = C_2 e^{rt} \\ \Rightarrow \frac{1-x}{x} &= \frac{1}{C_2 e^{rt}} = C_3 e^{-rt} \\ \Rightarrow x(t) &= \frac{1}{C_3 e^{-rt} + 1} \end{aligned}$$

Let the initial state at $t = 0$ be x_0 ,

$$\text{Then } C_3 = \frac{1}{x_0} - 1; \quad \text{and } x_0 < 1 \rightarrow C_3 > 0$$

$$\text{If } \frac{x}{1-x} < 0 \rightarrow x < 0 \quad \text{or } x > 1$$

$$\Rightarrow x(t) = \frac{1}{-C_4 e^{-rt} + 1}, \quad C_4 = 1 - \frac{1}{x_0}$$

$$\Rightarrow x(t) = \frac{1}{C e^{-rt} + 1}, \quad C = \left| \frac{1}{x_0} - 1 \right|$$

$$C_1, C_2, C_3, C_4 \text{ and } C \text{ are constants.} \quad (12)$$

The dynamical characteristics of the continuous logistic function are very similar to those of the integrate-and-fire model ($\dot{v} = b - v$). Fig. 13 depicts the time responses of the logistic function with different parameters (r , v_{peak} , v_{reset}) in the $v(t) - t$ plots. The solution of the differential equation

$v(t)$ is plotted in red, and the $v(t)$ generated with boundary conditions v_{peak} and v_{reset} using Euler method is plotted in blue. The initial value $x_0 = 0.1$. The initial value cannot be set to 0 as it cannot be used to calculate the value of constant C_3 in (12). In order to generate periodic spikes, the upper boundary v_{peak} of the spiking train can only be less than 1, as $v(\infty)$ asymptotes to 1 but will never reach 1.

$$\begin{aligned} \dot{v} &= \frac{dv}{dt} = b - v + v^2 \\ \therefore (v - \frac{1}{2})^2 &= v^2 - v + \frac{1}{4} \\ \Rightarrow \frac{dv}{dt} &= (v - \frac{1}{2})^2 + b - \frac{1}{4} \\ \text{Let } x = v - \frac{1}{2}, b' = b - \frac{1}{4} \\ \Rightarrow \frac{dx}{dt} &= \frac{dv}{dt} = x^2 + b' \text{ (quadratic form)} \\ \Rightarrow x(t) &= \sqrt{b'} * \tan \left(\sqrt{b'} * (t + C) \right) \\ \Rightarrow v(t) &= x(t) + \frac{1}{2} \\ &= \sqrt{b - \frac{1}{4}} * \tan \left(\sqrt{b - \frac{1}{4}} * (t + C) \right) + \frac{1}{2} \\ \text{Let } v(0) = v_0, \\ \text{Then } C &= \frac{1}{\sqrt{b - \frac{1}{4}}} \text{atan} \frac{v_0 - \frac{1}{2}}{\sqrt{b - \frac{1}{4}}} \end{aligned}$$

The period of the spiking:

$$T = \frac{1}{\sqrt{b - \frac{1}{4}}} \left(\text{atan} \frac{v_{peak}}{\sqrt{b - \frac{1}{4}}} - \text{atan} \frac{v_{reset}}{\sqrt{b - \frac{1}{4}}} \right) \quad (13)$$

The logistic function has a common ‘S’ shape. In fact, the sigmoid function, which is a prevalently used activation function for building conventional neuron model, is indeed a special case of the logistic function [16]. The rising speed of the spike depends on parameter r . The bigger r is, the faster $v(t)$ ramps from v_{reset} to v_{peak} , and hence the faster the spiking frequency is.

C. USING CONTINUOUS LOGISTIC FUNCTION TO APPROXIMATE DISCRETE LOGISTIC MAP

The solution to the differential equation of the continuous logistic function $x(t)$ can be used to approximate the outputs of the discrete logistic map $x(n)$. The sequential discrete values of the logistic map are used as the initial values x_0 for the logistic function to calculate the constant value C and the following output, with a time step dt , that is, $C = |\frac{1}{x_0} - 1|$, $x(t) = 1/(Ce^{-rt} + 1)$. Fig. 15 shows the chaotic outputs of the discrete logistic map ($x_0 = 0.2$, $r = 4$), and the approximations of the continuous logistic function $x(t)$ using different time steps (dt). It can be observed that the approximation is accurate when dt is small enough, in this case, the approximation is plausible when $dt = 0.01$.

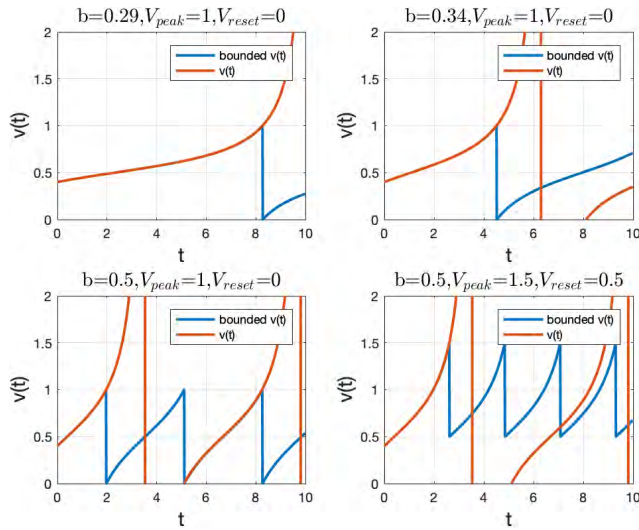
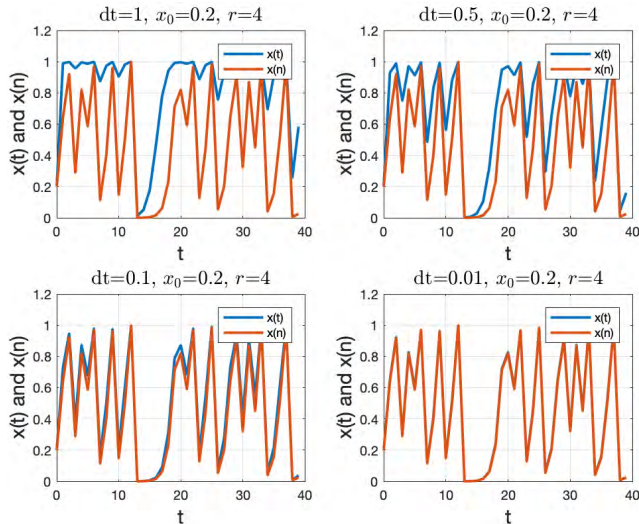
FIGURE 14. Parameters of logistic spiking model ($r = -1$).

FIGURE 15. Discrete logistic map approximated by continuous logistic function.

IV. LOGISTIC SPIKING NEURON MODEL

A. LOGISTIC SPIKING NEURON MODEL WITH $R = -1$

It can be observed from (12) that if $r = -1$, the equation becomes $\dot{x} = -x + x^2$. By substituting x with v , and adding a parameter b , this equation becomes $\dot{v} = 2b - v + v^2$, which is the summation of the integrate-and-fire model ($\dot{v} = b - v$) and the quadratic integrate-and-fire model ($\dot{v} = b + v^2$). The term $2b$ can be replaced by b to obtain a normal form for the equation. The steps for deriving the general solution to the differential equation of the logistic spiking neuron model, and the period (T) are of the spiking are listed in (13).

The dynamical characteristics of the logistic spiking neuron model are very similar to those of the quadratic integrate-and-fire model ($\dot{v} = b + v^2$). Fig. 14 depicts the time responses of the logistic spiking model with different parameters (b, v_{peak}, v_{reset}) in the $v(t) - t$ plots. The solution of

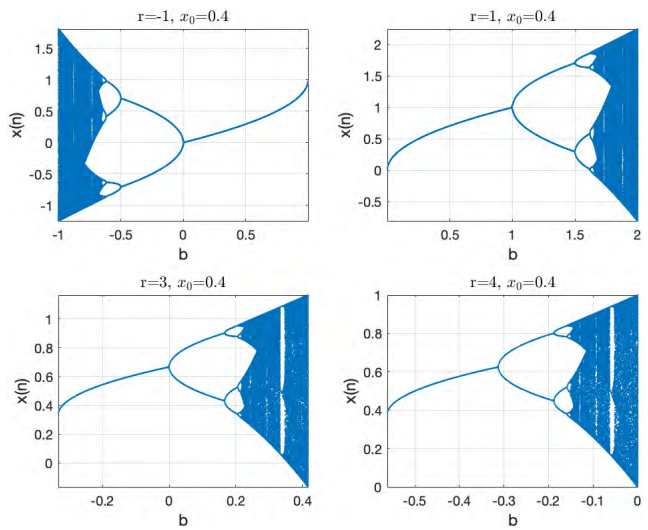


FIGURE 16. Bifurcation for discrete logistic spiking model - b.

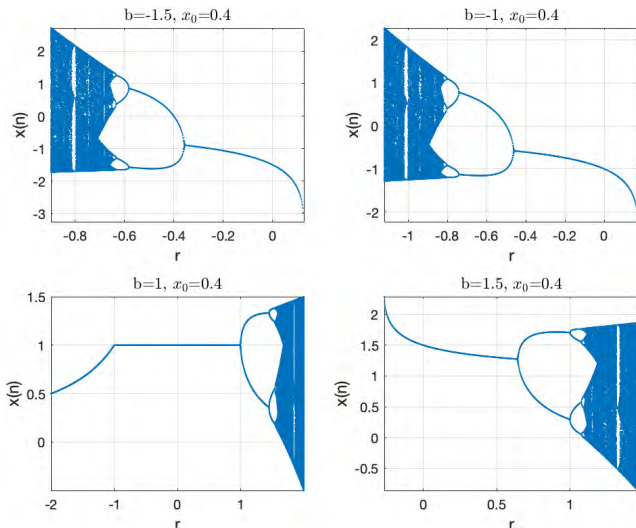
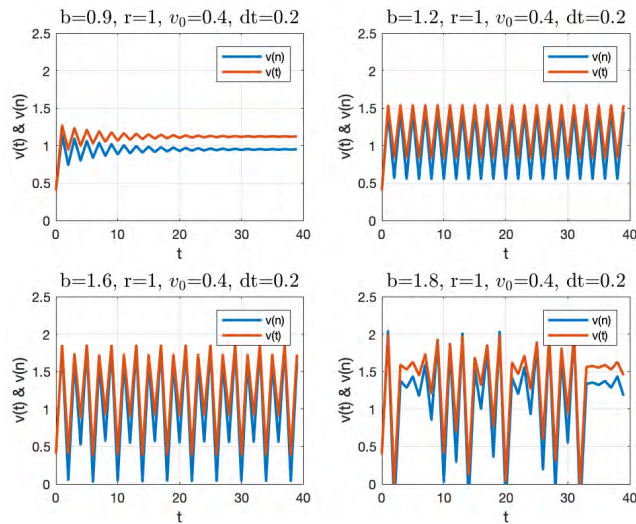
the differential equation $v(t)$ is plotted in red, and the $v(t)$ generated with boundary conditions v_{peak} and v_{reset} using Euler method is plotted in blue. The initial value $x_0 = 0.4$.

B. GENERALIZED LOGISTIC SPIKING NEURON MODEL

In a spiking neuron model, the parameter b can represent the input current to the neuron from post-synaptic spiking or external stimulus. It can be used to manipulate the dynamical behaviors of a spiking neuron model. The parameter r controls the rising speed of the slope. Unlike parameter b , it is related to a spiking neuron's intrinsic behaviors and internal activities such as the conductance of ion channels. Therefore, it depends on the neuron type and should not be used as a dynamical control parameter in the simulation of a spiking neuron model. The differential equation and its solution of the generalized logistic spiking neuron model are listed in (14).

$$\begin{aligned} \dot{v} &= b + rv - rv^2 \\ r - 2A * \tan \left(A(t + \frac{\arctan(\frac{r-2rv_0}{2A})}{A}) \right) \\ v(t) &= \frac{\sqrt{-r^2 - br}}{2r} \\ A &= \sqrt{\frac{-r^2}{4} - br} \end{aligned} \quad (14)$$

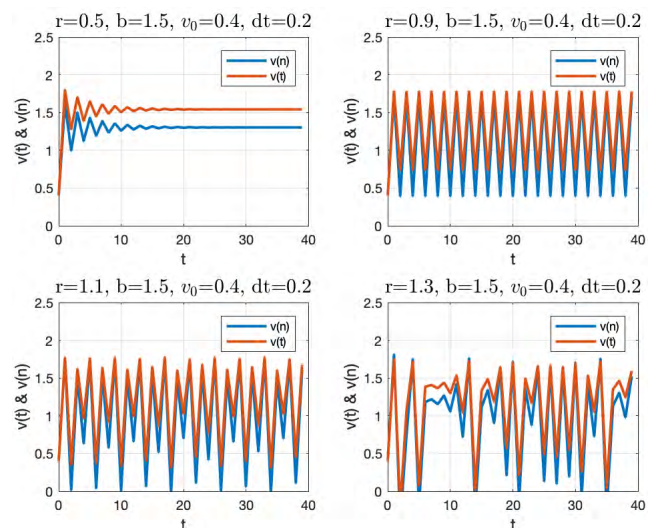
Analytically, both parameter b and r can be used to control the logistic spiking neuron model to be at stable, periodic or chaotic state; or go through period doubling towards chaotic by continuously increasing or decreasing the parameter. When considered as a modified model for the discrete logistic map, the bifurcations over parameter b for four r values ($r = -1, 1, 3, 4$) are plotted in Fig. 16, with initial value $v_0 = 0.4$. In the case in Fig. 16 (top right), where $r = 1$, $v_0 = 0.4$, when $0 < b < 1$, $v(n)$ converges to a stable value; when $1 < b < 1.5$, $v(n)$ oscillates periodically between two stable values; as b increases from 1.5 to 2, $v(n)$ quickly

**FIGURE 17.** Bifurcation for discrete logistic spiking model - r.**FIGURE 18.** Parameter b of the logistic spiking model ($r = 1$).

goes through period doubling towards chaotic. This is further illustrated by Fig. 18, which shows the discrete $v(n)$ and the approximation of continuous $v(t)$ with four different b values. With the same setting for all other parameters: $r = 1, v_0 = 0.4, dt = 0.2$:

- When $b = 0.9$ (top left), $v(n)$ converges to a stable value;
- When $b = 1.2$ (top right), $v(n)$ oscillates periodically between two values;
- When $b = 1.6$ (bottom left), $v(n)$ alternates sequentially and periodically among four values;
- When $b = 1.8$ (bottom right), $v(n)$ becomes chaotic.

Similarly, the bifurcations over parameter r for four different b values ($b = -1.5, -1, 1, 1.5$) are plotted in Fig. 17, also with initial value $v_0 = 0.4$. The example in Fig. 17 (bottom right) with $b = 1.5$ is further illustrated by Fig. 19, which shows the discrete $v(n)$ and the approximation of continuous $v(t)$ at four different r values. With the same setting for all other parameters: $b = 1.5, v_0 = 0.4, dt = 0.2$:

**FIGURE 19.** Parameter r of the logistic spiking model ($b = 1.5$).

- When $r = 0.5$ (top left), $v(n)$ converges to a stable value;
- When $r = 0.9$ (top right), $v(n)$ oscillates periodically between two values;
- When $r = 1.1$ (bottom left), $v(n)$ alternates sequentially and periodically among four values;
- When $r = 1.3$ (bottom right), $v(n)$ becomes chaotic.

A more accurate approximation of $v(t)$ can be achieved by using a smaller value for the time step $dt = 0.01$.

V. CONCLUSION AND FOLLOWING RESEARCH

Building the novel logistic spiking model discussed in this paper is inspired by the integrate-and-fire as well as the quadratic integrate-and-fire spiking neuron models. The combination of these two well-studied spiking neuron models resembles the mathematical representation of the discrete logistic map, which is a very plausible model for analyzing the dynamics of a natural system such as the population growth of a species. It has been demonstrated that the mathematically derived solution $v(t)$ to the continuous differential logistic function can be used to approximate the corresponding discrete logic map accurately with a small increment time step. This can also be applied to the discrete and continuous representations of the novel spiking neuron model, which includes an additional parameter (b) to simulate an external current input to the spiking neuron model. The added parameter can effectively control the stability of the neuron dynamics, which also depends on the neural intrinsic parameter (r). The analytical approach presented here can be utilized for the dynamical analyses of one dimensional spiking neuron models in particular, and extensively for multi-dimensional spiking neuron models in general, which will be included in the following research. The designed logistic spiking neural model can be used for studying brain dynamics and building artificial intelligence in general. A specific application for the research outcome is to use brain stimulation to treat

movement related cognitive disorder such as epilepsy and Parkinson's Disease. This requires long-term data collection using electroencephalogram (EEG) or functional magnetic resonant imaging (fMRI) from patients in clinical setup, which will be endeavored in the follow up research.

REFERENCES

- [1] E. M. Izhikevich, "Simple model of spiking neurons," *IEEE Trans. Neural Netw.*, vol. 14, no. 6, pp. 1569–1572, Nov. 2003.
- [2] S. Hashimoto and H. Torikai, "A novel hybrid spiking neuron: Bifurcations, responses, and on-chip learning," *IEEE Trans. Circuits Syst. I, Reg. Papers*, vol. 57, no. 8, pp. 2168–2181, Aug. 2010.
- [3] G. Wulfram and W. M. Kistler, *Spiking Neuron Models*. Cambridge, U.K.: Cambridge Univ. Press, 2002.
- [4] G. Boeing, "Visual analysis of nonlinear dynamical systems: Chaos, fractals, self-similarity and the limits of prediction," *Systems*, vol. 4, no. 37, p. 37, Nov. 2016.
- [5] L. P. Maguire, T. M. McGinnity, B. Glackin, A. Ghani, A. Belatreche, and J. Harkin, "Challenges for large-scale implementations of spiking neural networks on FPGAs," *Neurocomputing*, vol. 71, nos. 1–3, pp. 13–29, Dec. 2007.
- [6] L. Zhang, "Design and implementation of neural network based chaotic system model for the dynamical control of brain stimulation," in *Proc. 2nd Int. Conf. Neurosci. Cognit. Brain Inf.*, Nice, France, Jul. 2017, pp. 14–21.
- [7] L. Zhang, "Artificial neural network architecture design for EEG time series simulation using chaotic system," in *Proc. 7th Int. Conf. Inform., Electron. Vis. (ICIEV)*, Jun. 2018, pp. 388–393.
- [8] L. Zhang, "Evaluating the training performance of artificial neural network using small time series segments of the lorenz chaotic system," in *Proc. Int. Joint Conf. Neural Netw. (IJCNN)*, Jul. 2018, pp. 1–8.
- [9] L. Zhang, "Optimizing ANN training performance for chaotic time series prediction using small data size," *Int. J. Mach. Learn. Comput.*, vol. 8, no. 6, pp. 606–612, Dec. 2018.
- [10] L. Zhang, "Improving the efficacy of artificial neural network training by optimizing training data for the simulation and prediction of electroencephalogram chaotic patterns," in *Proc. 17th IEEE Int. Conf. Cognit. Informat. Cognit. Comput. (ICCIICC)*, Jul. 2018, pp. 145–153.
- [11] S. Lynch and J. Borresen, "Binary half-adder using oscillators," U.S. Patent 20130093458 A1, Jun. 1, 2015.
- [12] S. Lynch, J. Borresen, and K. Latham, "Josephson junction binary oscillator computing," in *Proc. IEEE 14th Int. Superconductive Electron. Conf. (ISEC)*, Jul. 2013, pp. 1–3.
- [13] E. M. Izhikevich, *Dynamical Systems in Neuroscience: The Geometry of Excitability and Bursting (Computational Neuroscience)*. Cambridge, MA, USA: MIT Press, 2006.
- [14] A. L. Hodgkin and A. F. Huxley, "A quantitative description of membrane current and its application to conduction and excitation in nerve," *J. Physiol.*, vol. 117, no. 4, pp. 500–544, 1952.
- [15] E. W. Weisstein. *Logistic Equation, MathWorld-A Wolfram Web Resource*. Accessed: Apr. 2019. [Online]. Available: <http://mathworld.wolfram.com/LogisticEquation.html>
- [16] T. M. Mitchell, *Machine Learning*. New York, NY, USA: McGraw-Hill, 1997, ch. 4, pp. 96–97.



LEI ZHANG (M'06) was born in Qingdao, China. She received the bachelor's degree in electrical and electronic engineering from Qingdao University, China, in 2003, the master's degree in electrical and electronic engineering from Durham University, U.K., in 2006, and the Ph.D. degree in electrical and electronic engineering from Brunel University, U.K., in 2012.

She has been an Assistant Professor with the Faculty of Engineering and Applied Science, University of Regina, Canada, since 2013. Prior to her academic career, she was a Project Leader and an Electronic Design Engineer with TWI Ltd., U.K., from 2006 to 2012, and a Senior Hardware Engineer and Consultant with the Cambridge Technology Group, U.K., in 2013. She is a registered Professional Engineer (PEng.) with the Association of Professional Engineers and Geoscientists (APEGS) in Canada, a registered Chartered Engineer (CEng) with the British Engineering Council, and a registered European Engineer (Eur ING) with the European Federation of National Engineering Associations. She is passionate about teaching, research, and innovation, as well as philosophy, history, and music.